

LLM4TS: Aligning Pre-Trained LLMs as Data-Efficient Time-Series Forecasters

Ching Chang, Wei-Yao Wang, Wen-Chih Peng and Tien-Fu Chen

National Yang Ming Chiao Tung University, Hsinchu, Taiwan

blacksnail789521.cs10@nycu.edu.tw, sf1638.cs05@nctu.edu.tw, {wcpeng, tfchen}@cs.nycu.edu.tw

Abstract

Multivariate time-series forecasting is vital in various domains, e.g., economic planning and weather prediction. Deep train-from-scratch models have exhibited effective performance yet require large amounts of data, which limits real-world applicability. Recently, researchers have explored pre-trained Large Language Models (LLMs) for limited non-linguistic datasets. However, incorporating LLMs with time-series data presents challenges of limited adaptation due to different compositions between time-series and linguistic data, and the inability to process multi-scale temporal information. To tackle these challenges, we propose LLM4TS, a framework for time-series forecasting with pre-trained LLMs. LLM4TS consists of a two-stage fine-tuning strategy: the *time-series alignment* stage to align LLMs with the nuances of time-series data, and the *forecasting fine-tuning* stage, which is specifically designed for time-series forecasting tasks. Furthermore, our framework features a novel two-level aggregation method that integrates multi-scale temporal data within pre-trained LLMs, enhancing their ability to interpret time-specific information. In experiments across 7 time-series forecasting datasets, LLM4TS is superior to existing state-of-the-art methods, including those trained from scratch, in full-shot scenarios, and also achieves an average improvement of 6.84% in MSE in few-shot scenarios. In addition, evaluations compared with different self-supervised learning approaches highlight LLM4TS’s effectiveness with representation learning in forecasting scenarios.

1 Introduction

Forecasting is a vital task in multivariate time-series analysis, not only for its ability to operate without manual labeling but also for its importance in practical applications such as economic planning [Lai *et al.*, 2018] and weather prediction [Zhou *et al.*, 2021]. Recently, numerous methods have been developed for time-series forecasting [Zeng *et al.*, 2023; Nie *et al.*, 2023], although some lean towards unsupervised representation learning [Chang *et al.*, 2023] and transfer

learning [Zhang *et al.*, 2022; Zhou *et al.*, 2023]. Generally, these approaches aim to employ adept representation learners: first extracting rich representations from the time-series data and then using these representations for forecasting.

Achieving an adept representation learner requires sufficient training data [Hoffmann *et al.*, 2022], yet in real-world scenarios, there is often a lack of large-scale time-series datasets. For instance, in industrial manufacturing, the sensor data for different products cannot be combined for further analysis, leading to limited data for each product type [Yeh *et al.*, 2019]. Recent research has pivoted towards pre-trained LLMs in Natural Language Processing (NLP) [Radford *et al.*, 2019; Touvron *et al.*, 2023], exploiting their robust representation learning and few-shot learning capabilities. Moreover, these LLMs can adapt to non-linguistic datasets (e.g., images [Lu *et al.*, 2021], audio [Ghosal *et al.*, 2023], tabular data [Hegselmann *et al.*, 2023], and time-series data [Zhou *et al.*, 2023]) by fine-tuning with only a few parameters and limited data. While LLMs are renowned for their exceptional transfer learning capabilities across various fields, the domain-specific nuances of time-series data introduce two challenges in leveraging these models for time-series forecasting.

The first challenge of employing LLMs for time-series forecasting is their limited adaptation to the unique characteristics of time-series data due to LLMs’ initial pre-training focus on the linguistic corpus. While LLMs have been both practically and theoretically proven [Zhou *et al.*, 2023] to be effective in transfer learning across various modalities thanks to their data-independent self-attention mechanism, their primary focus on general text during pre-training causes a shortfall in recognizing key time-series patterns and nuances crucial for accurate forecasting. This limitation is evident in areas such as meteorology and electricity forecasting [Zhou *et al.*, 2021], where failing to account for weather patterns and energy consumption trends leads to inaccurate predictions.

The second challenge lies in the limited capacity to process multi-scale temporal information. While LLMs are adept at understanding the sequence and context of words, they struggle to understand temporal information due to the lack of utilizing multi-scale time-related data such as time units (e.g., seconds, minutes, hours, etc.) and specific dates (e.g., holidays, significant events). This temporal information is vital in time-series analysis for identifying and predicting patterns [Wu *et al.*, 2021]; for instance, in energy management, it is

used to address consumption spikes during daytime and in summer/winter, in contrast to the lower demand during the night and in milder seasons [Zhou *et al.*, 2021]. This underscores the importance of models adept at interpreting multi-scale temporal patterns (hourly to seasonal) for precise energy demand forecasting. However, most LLMs (e.g., [Radford *et al.*, 2019; Touvron *et al.*, 2023]) built on top of the Transformer architecture do not naturally incorporate multi-scale temporal information, leading to models that fail to capture crucial variations across different time scales.

To address the above issues, we propose LLM4TS, a framework for time-series forecasting with pre-trained LLMs (as illustrated in Figure 1). Regarding the first challenge, our framework introduces a two-stage fine-tuning approach: the *time-series alignment* stage and the *forecasting fine-tuning* stage. The first stage focuses on aligning the LLMs with the characteristics of time-series data by utilizing the autoregressive objective, enabling the fine-tuned LLMs to recognize time-series patterns and nuances essential for precise forecasting. Subsequently, the second stage is incorporated to learn corresponding time-series forecasting tasks. In this manner, our model can support effective performance in full- and few-shot scenarios. Notably, throughout both stages, most parameters in the pre-trained LLMs are kept fixed, maintaining the model’s inherent representation learning capability. To overcome the limitation of LLMs in integrating multi-scale temporal information, we introduce a novel two-level aggregation strategy. This approach embeds multi-scale temporal information directly into the patched time-series data, ensuring that each patch not only represents the series values but also encapsulates the critical time-specific context.

In summary, the primary contributions of this paper are listed as follows:

- **Aligning LLMs toward Time-Series Data:** To the best of our knowledge, LLM4TS is the first method to align pre-trained LLMs with time-series characteristics with the proposed *time-series alignment* stage.
- **Multi-Scale Temporal Information in LLMs:** We propose a two-level aggregation method to integrate multi-scale temporal data within pre-trained LLMs, enhancing their ability to interpret time-specific information.
- **Outstanding Performance in Forecasting:** LLM4TS excels in 7 real-world time-series forecasting benchmarks, outperforming state-of-the-art methods, including those trained from scratch. It also demonstrates strong few-shot capabilities, particularly with only 5% of data, where it surpasses the best baseline that uses 10% of data. This efficiency makes LLM4TS highly relevant for practical, real-world forecasting applications.

2 Related Work

2.1 Transfer Learning Across Various Modalities with LLMs

LLMs have demonstrated their effectiveness in transfer learning across a variety of modalities, such as images [Lu *et al.*, 2021], audio [Ghosal *et al.*, 2023], tabular data [Hegselmann *et al.*, 2023], and time-series data [Zhou *et al.*, 2023]. A

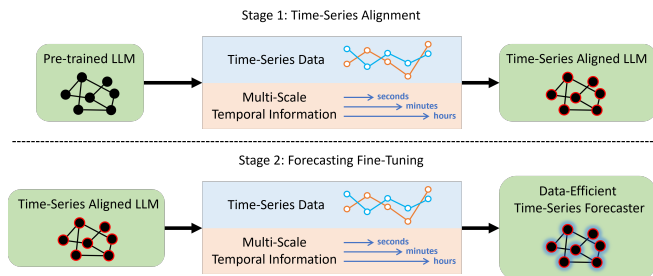


Figure 1: We first align a pre-trained LLM with the time-series characteristics, and then fine-tune it for the time-series forecasting task. Throughout both stages, we integrate multi-scale temporal information while keeping most parameters in the LLM fixed.

key motivation for employing LLMs in various modalities is their ability to achieve notable performance with limited data [Zhou *et al.*, 2023]. To preserve their data-independent representation learning capability, most parameters in these LLMs are kept fixed. Empirical evidence [Lu *et al.*, 2021; Zhou *et al.*, 2023] indicates that LLMs keeping most parameters unchanged often outperform those trained from scratch, underscoring the value of maintaining these models’ pre-existing representation learning strengths. Theoretically, it is shown that the self-attention modules in these pre-trained transformers develop the capacity for data-independent operations (akin to principal component analysis [Zhou *et al.*, 2023]), enabling them to function effectively as general computation calculators [Giannou *et al.*, 2023]. In the time-series domain, GPT4TS [Zhou *et al.*, 2023] utilizes the pre-trained GPT-2 and demonstrates strong performance in time-series forecasting under few-shot conditions without modifying most parameters. With our LLM4TS, we address the challenges of limited adaptation to time-series characteristics and the difficulty in processing multi-scale temporal information, thereby enhancing performance in time-series forecasting.

2.2 Long-term Time-Series Forecasting

Numerous efforts have been dedicated to employing Transformer models for long-term time-series forecasting [Zhou *et al.*, 2021; Wu *et al.*, 2021; Zhou *et al.*, 2022; Nie *et al.*, 2023]. While Transformer-based models have gained traction, DLin-ear [Zeng *et al.*, 2023] reveals that a single-layer linear model can surpass many of these sophisticated Transformer-based approaches. These deep train-from-scratch models exhibit outstanding performance when trained on sufficient datasets, but their efficacy decreases in limited-data scenarios. In contrast, LLM4TS sets new benchmarks alongside these state-of-the-art approaches in both full- and few-shot scenarios.

2.3 Time-Series Representation Learning

In the time-series domain, self-supervised learning emerges as a prominent approach to representation learning. While Transformers are widely recognized as prime candidates for end-to-end time-series analysis [Xu *et al.*, 2021; Liu *et al.*, 2021; Nie *et al.*, 2023], CNN-based [Yue *et al.*, 2022] or RNN-based [Tonekaboni *et al.*, 2021] backbones consistently stand out as the preferred architecture in time-series self-supervised learning. However, the inherent capability of

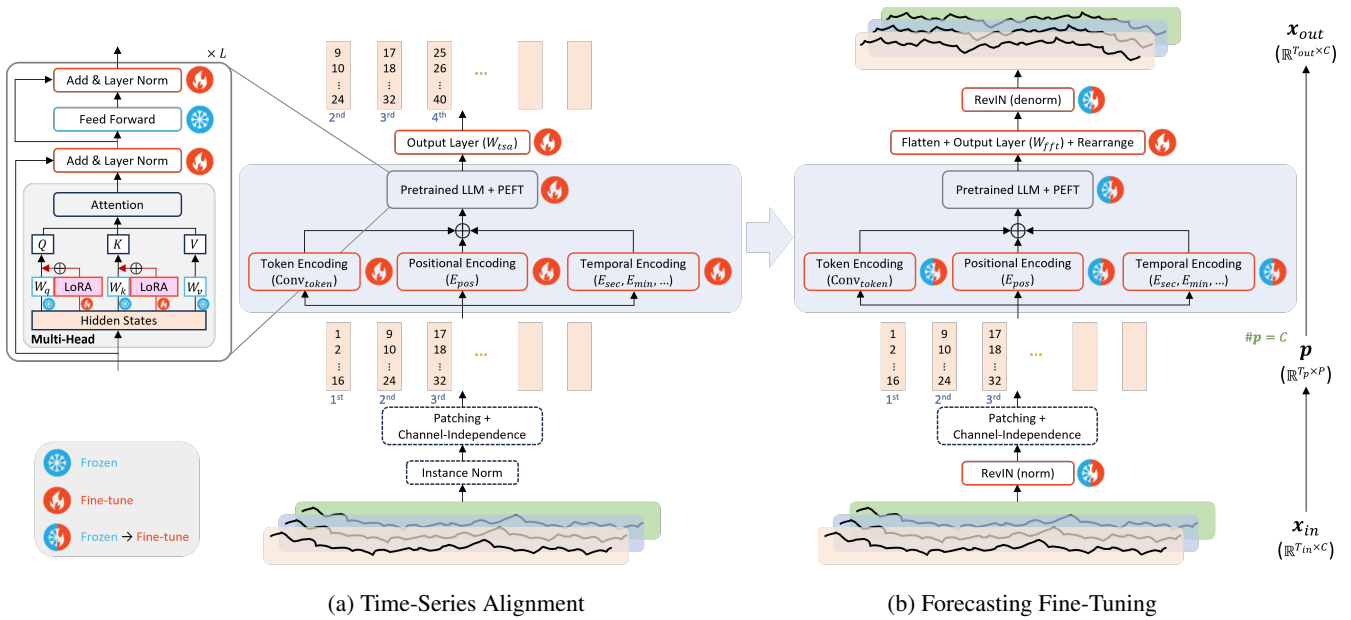


Figure 2: LLM4TS framework. The numbers in the patched time series (e.g., 1, 2, ..., 16 in the first patch) indicate the sequential order of the timestamps. The framework consists of two stages: (a) Time-series alignment, which uses the autoregressive approach to align the pre-trained LLM with patched time-series data. (b) Forecasting fine-tuning, which starts with linear probing (i.e., only the output layer is unfrozen), followed by full fine-tuning (all the layers and PEFT components in the LLM are unfrozen).

Transformers to model long-range dependencies and capture patterns aligns perfectly with time-series data, which involve complex sequential relationships. Since the *time-series alignment* stage in LLM4TS can be seen as a self-supervised learning approach, we evaluate LLM4TS’s representation learning capability and demonstrate the full potential of Transformers in self-supervised learning, surpassing the performance of conventional CNN and RNN-based models.

3 Problem Formulation

Given a complete and evenly-sampled multivariate time series, we use a sliding data window to extract sequential samples. This window moves with a stride of 1 and has a total length of $T_{in} + T_{out}$ — comprising past data $\mathbf{x}_{in} = (d_1, \dots, d_{T_{in}})$ with a look-back window length T_{in} and future data $\mathbf{x}_{out} = (d_{T_{in}+1}, \dots, d_{T_{in}+T_{out}})$ with a prediction length T_{out} . For each time step t , d_t represents a C -dimensional vector, where C denotes the number of features. Our objective is to use the past data $\mathbf{x}_{in} \in \mathbb{R}^{T_{in} \times C}$ to predict the future data $\mathbf{x}_{out} \in \mathbb{R}^{T_{out} \times C}$.

4 The Proposed LLM4TS

Figure 2 illustrates our LLM4TS framework, leveraging the pre-trained GPT-2 [Radford *et al.*, 2019] as the backbone model. We first introduce the time-series alignment stage, which focuses on aligning the LLMs with the characteristics of time-series data using an autoregressive objective (Section 4.1). Subsequently, the forecasting fine-tuning stage is designed to further enhance the model’s ability to handle time-series forecasting tasks (Section 4.2).

4.1 Time-Series Alignment

Existing LLMs are pre-trained on a general language corpus, which means they fail to learn contextualized information outside linguistic domains; therefore, the *time-series alignment* stage is proposed to align LLMs with the characteristics of time-series data. Given our selection of GPT-2 [Radford *et al.*, 2019] as the backbone model, which is a causal language model, we ensure that this stage adopts the same *autoregressive* training methodology used during its pre-training phase. Figure 2(a) illustrates the autoregressive objective in the time-series alignment stage: given an input sequence of patched time-series data (e.g., 1st patch, 2nd patch, 3rd patch, etc.), the backbone model generates an output sequence shifted one patch to the right (e.g., 2nd patch, 3rd patch, 4th patch, etc.).

Instance Normalization

Data normalization is essential for stable performance when adapting pre-trained models across various modalities. Alongside the layer normalization used in the pre-trained LLM, we incorporate instance normalization to improve consistency and reliability in handling diverse time-series datasets. In our model, instance normalization is employed without incorporating a trainable affine transformation. This is crucial because when a batch of data is gathered and instance normalization is applied with a trainable affine transformation, the resulting transformed data becomes unsuitable to be the ground truth for the output. Given that an autoregressive objective is used at this stage, applying a trainable affine transformation is not feasible.

Given an input time-series sample $\mathbf{x}_{in} \in \mathbb{R}^{T_{in} \times C}$, we apply instance normalization (IN) to produce a normalized time-series sample $\mathbf{x}_{normed} \in \mathbb{R}^{T_{in} \times C}$ with zero mean and

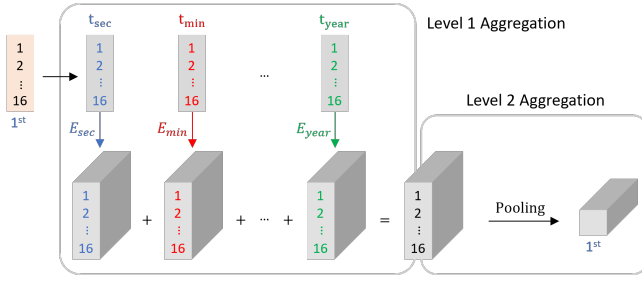


Figure 3: Temporal encoding for patched time-series data involves a two-level aggregation process. In this figure, only the first patch is shown for simplicity, but in practice, all patches in a batch are processed simultaneously. Level 1 aggregation calculates the temporal embedding for each time unit and sums them together. Next, Level 2 aggregation applies a pooling method to extract the final temporal embedding \mathbf{e}_{temp} .

unit standard deviation:

$$\mathbf{x}_{normed} = \text{IN}(\mathbf{x}_{in}). \quad (1)$$

Time-Series Tokenization

The context window sizes in pre-trained LLMs (e.g., 1024 in GPT-2) are sufficient for NLP tasks but are inadequate for long-term time-series forecasting. In our experiments, a prediction length of 720 combined with a look-back window size of 512 easily exceeds these limits. To address this, we adopt *channel-independence* along with *patching* [Nie *et al.*, 2023] for time-series tokenization, effectively resolving the context window size constraint and simultaneously reducing the time and space complexity of the Transformer quadratically. Channel-independence converts multivariate time-series data into multiple univariate time-series data, thus transforming the data’s dimension to $\mathbb{R}^{T_{in} \times 1}$, with the channel dimension C merged into the batch size dimension. The subsequent patching step groups adjacent time steps into a singular patch-based token, reducing the input sample’s time dimension from T_{in} to T_p , where T_p denotes the number of patches, and concurrently expanding the feature dimension from 1 to P , with P representing the patch length.

Given a normalized time-series sample $\mathbf{x}_{normed} \in \mathbb{R}^{T_{in} \times C}$, we first apply channel-independence (CI), and then patching to produce a series of patches $\mathbf{p} \in \mathbb{R}^{T_p \times P}$:

$$\mathbf{p} = \text{patching}(\text{CI}(\mathbf{x}_{normed})). \quad (2)$$

Three Encodings for Patched Time-Series Data

Given our goal to adapt a pre-trained LLM for time-series data, the original token encoding layer (designed for text) becomes unsuitable due to the mismatched modalities. Additionally, we design a new temporal encoding layer to address the inability to process multi-scale temporal information.

Given a series of tokens, applying token encoding is necessary to align their dimensions with the latent embedding dimension of the pre-trained LLM. In standard NLP practices, this encoding uses a trainable lookup table to map tokens into a high-dimensional space. However, this method only suits *scalar* tokens, whereas our patched time-series data are *vectors*. Therefore, we drop the original token encoding layer in

the LLM, and employ a one-dimensional convolutional layer Conv_{token} as our new token encoding layer. As opposed to employing a linear layer [Zhou *et al.*, 2023], we choose a convolutional layer due to its superior ability to retain local semantic information within the time-series data. This results in the generation of the token embedding $\mathbf{e}_{token} \in \mathbb{R}^{T_p \times D}$, where D denotes the dimension of the embeddings:

$$\mathbf{e}_{token} = \text{Conv}_{token}(\mathbf{p}). \quad (3)$$

For the positional encoding layer, we employ a trainable lookup table E_{pos} to map patch locations. This results in the generation of the positional embedding $\mathbf{e}_{pos} \in \mathbb{R}^{T_p \times D}$:

$$\mathbf{e}_{pos} = E_{pos}(\mathbf{i}), \quad (4)$$

where $\mathbf{i} \in \mathbb{R}^{T_p}$ represents the indices of the patch locations.

To address the challenge LLMs face in processing multi-scale temporal information, we introduce a temporal encoding layer. When processing time-related data, we face two challenges due to the need to aggregate multiple pieces of information into one unified representation (Figure 3):

1. Each timestamp includes a range of multi-scale temporal attributes (e.g., seconds, minutes, hours, holidays, etc.).
2. Each patch encompasses multiple timestamps.

To address the first challenge associated with diverse temporal attributes within a timestamp, we employ Level 1 aggregation: a trainable lookup table for each temporal attribute (e.g., E_{sec}, E_{min}, \dots), mapping it into a high-dimensional space, and then summing them to produce a singular temporal embedding. In response to the second challenge of multiple timestamps within a patch, we use Level 2 aggregation: a pooling method to extract the final temporal embedding. For the pooling method, we opt for the “select first” method, where the initial timestamp is designated as representative of the entire patch. This is because the first timestamp often carries the most significant and representative information for the entire duration covered by the patch, especially in time-series data where earlier events can have a substantial influence on the subsequent sequence. This process generates the final temporal embedding $\mathbf{e}_{temp} \in \mathbb{R}^{T_p \times D}$:

$$\mathbf{e}_{temp} = \text{Pooling} \left(\sum_{a \in \{\text{sec}, \text{min}, \text{hour}, \dots\}} E_a(\mathbf{t}_a) \right), \quad (5)$$

where a represents different temporal attributes (seconds, minutes, hours, holidays, etc.), E_a denotes the trainable lookup table for each temporal attribute, $\mathbf{t}_a \in \mathbb{R}^{T_p \times P}$ are the series of patches containing temporal information for that temporal attribute, and Pooling applies the pooling method to the aggregated embeddings.

Finally, the token, positional, and temporal embeddings are summed to yield the final embedding $\mathbf{e} \in \mathbb{R}^{T_p \times D}$, which is then fed into the pre-trained Transformer blocks:

$$\mathbf{e} = \mathbf{e}_{token} + \mathbf{e}_{pos} + \mathbf{e}_{temp}. \quad (6)$$

Pre-Trained LLM

To preserve LLMs’ data-independent representation learning capability, most parameters in these LLMs are kept fixed.

Empirical evidence [Lu *et al.*, 2021; Zhou *et al.*, 2023] shows that training these LLMs from scratch often hurts performance, highlighting the importance of fixing most parameters to retain the LLM’s representation learning capability. To that end, we opt for freezing most parameters, particularly those associated with the multi-head attention and feed-forward layers in the Transformer block, as they are the most responsible for representation learning [Zhou *et al.*, 2023].

For the remaining trainable parameters in the pre-trained LLM, we employ two Parameter-Efficient Fine-Tuning (PEFT) methods to selectively adjust or introduce a limited set of trainable parameters. Specifically, we utilize Layer Normalization Tuning [Lu *et al.*, 2021] to adjust pre-existing parameters in Transformer blocks, making the affine transformation in layer normalization trainable. Concurrently, we employ Low-Rank Adaptation (LoRA) [Hu *et al.*, 2021], which introduces trainable low-rank matrices that are applied to the query (Q) and key (K) matrices in the self-attention mechanism. With these two PEFT techniques, only 1.5% of the pre-trained LLM’s total parameters are used to be trained.

Given the embedding \mathbf{e} (which is adjusted to the required embedding dimension D by three encoding layers), we pass it into the pre-trained LLM, which comprises a series of pre-trained Transformer blocks (TBs) (with L blocks in total). This process yields the final embeddings $\mathbf{z} \in \mathbb{R}^{T_p \times D}$:

$$\mathbf{z} = \text{TBs}(\mathbf{e}). \quad (7)$$

After being processed by the pre-trained LLM, we employ a linear output layer $W_{tsa} \in \mathbb{R}^{P \times D}$ to transform the output embedding back to patched time-series data:

$$\hat{\mathbf{p}}_{shifted} = \mathbf{z}W_{tsa}^\top, \quad (8)$$

where $\hat{\mathbf{p}}_{shifted} \in \mathbb{R}^{T_p \times P}$ represents our prediction target, corresponding to the original time-series patches (\mathbf{p}) shifted one patch to the right, in line with the autoregressive objective of this stage. To ensure the prediction precisely reconstructs the actual shifted patched data $\mathbf{p}_{shifted} \in \mathbb{R}^{T_p \times P}$, we use the Mean Squared Error (MSE) as the loss function:

$$\mathcal{L}_{tsa} = \text{MSE}(\mathbf{p}_{shifted}, \hat{\mathbf{p}}_{shifted}). \quad (9)$$

4.2 Forecasting Fine-tuning

After aligning the pre-trained LLM with patched time-series data in the time-series alignment stage, we transfer the trained weights of the backbone model, including those from the encoding layers, to the *forecasting fine-tuning* stage. When fine-tuning the backbone model for the forecasting task, two primary training strategies are available: full fine-tuning (where all model parameters are updated) and linear probing (where only the final linear output layer is updated). Studies have shown that a sequential approach—initial linear probing followed by full fine-tuning (LP-FT, as illustrated in Figure 2(b))—consistently surpasses strategies exclusively employing either method [Kumar *et al.*, 2022]. The superiority of LP-FT is due to its dual-phase approach: first finding an optimized output layer to minimize later adjustments in fine-tuning (preserving feature extractor efficacy for out-of-distribution (OOD) scenarios), and then employing full fine-tuning to adapt the model to the specific task (enhancing in-distribution (ID) accuracy) [Kumar *et al.*, 2022].

Table 1: Statistical overview of the 7 datasets for long-term time-series forecasting.

Datasets	Features	Timesteps	Granularity
Weather	21	52,696	10 min
Traffic	862	17,544	1 hour
Electricity	321	26,304	1 hour
ETTh1 & ETTh2	7	17,420	1 hour
ETTm1 & ETTm2	7	69,680	5 min

For the model architecture in the forecasting fine-tuning stage, we preserve most of the structure as in the time-series alignment stage, including the three encoding layers and the pre-trained LLM. However, there are two architectural differences in this stage: instance normalization and the output layer.

The first architectural difference is in the instance normalization, where we adopt Reversible Instance Normalization (RevIN) [Kim *et al.*, 2021] to enhance forecasting accuracy. RevIN involves batch-specific instance normalization and subsequent denormalization, both sharing the same trainable affine transformation. The additional denormalization step addresses distribution shifts between training and testing data, which is a common challenge in the time-series domain (e.g., seasonal changes). Therefore, during the time-series tokenization step, we apply RevIN’s normalization, succeeded by channel-independence and patching:

$$\mathbf{p} = \text{patching}(\text{CI}(\text{RevIN}_{norm}(\mathbf{x}_{in}))). \quad (10)$$

Notably, the denormalization step is applicable only to unpatched time-series data; hence, in the time-series alignment stage, standard instance normalization is employed.

The second architectural difference lies in the output layer, whose function is to transform the final embedding \mathbf{z} into the predicted future data, presented in the general (unpatched) time-series format. This involves flattening the data and passing it through the linear output layer $W_{fft} \in \mathbb{R}^{T_{out} \times T_p \cdot D}$, followed by rearrangement, and then applying RevIN’s denormalization to obtain the final prediction $\hat{\mathbf{x}}_{out} \in \mathbb{R}^{T_{out} \times C}$:

$$\hat{\mathbf{x}}_{out} = \text{RevIN}_{denorm}(\text{Rearrange}((\text{Flatten}(\mathbf{z}))W_{fft}^\top)). \quad (11)$$

To ensure that this prediction accurately reconstructs the future data $\mathbf{x}_{out} \in \mathbb{R}^{T_{out} \times C}$, we use MSE as the loss function:

$$\mathcal{L}_{fft} = \text{MSE}(\mathbf{x}_{out}, \hat{\mathbf{x}}_{out}). \quad (12)$$

5 Experiments

Datasets We use 7 widely used multivariate time-series datasets to test our LLM4TS framework in long-term forecasting, including Weather, Traffic, Electricity, and 4 ETT sets (ETTh1, ETTh2, ETTm1, ETTm2). Detailed statistics for these datasets are provided in Table 1.

Baselines For long-term time-series forecasting, we focus on a range of state-of-the-art models. GPT4TS [Zhou *et al.*, 2023] is distinct in leveraging a pre-trained LLM (GPT-2), while DLinear [Zeng *et al.*, 2023], PatchTST [Nie *et al.*, 2023], FEDformer [Zhou *et al.*, 2022], Autoformer [Wu *et al.*, 2022],

Table 2: Long-term forecasting for multivariate time-series data. For all datasets, results are averaged over prediction lengths $T_{out} \in \{96, 192, 336, 720\}$. The best average results are in **bold**, while the second-best are underlined.

Methods	LLM4TS		GPT4TS		DLinear		PatchTST		FEDformer		Autoformer		Informer	
Metric	MSE	MAE	MSE	MAE	MSE	MAE	MSE	MAE	MSE	MAE	MSE	MAE	MSE	MAE
Weather	0.223	0.260	0.237	0.271	0.249	0.300	<u>0.226</u>	<u>0.264</u>	0.309	0.360	0.338	0.382	0.634	0.521
ETTh1	0.404	0.418	0.428	<u>0.426</u>	0.423	0.437	<u>0.413</u>	0.431	0.440	0.460	0.496	0.487	1.040	0.795
ETTh2	<u>0.333</u>	<u>0.383</u>	0.355	0.395	0.431	0.447	0.330	0.379	0.437	0.449	0.450	0.459	4.431	1.729
ETTh1	0.343	0.378	0.352	0.383	0.357	<u>0.379</u>	<u>0.351</u>	0.381	0.448	0.452	0.588	0.517	0.961	0.734
ETTh2	0.251	0.313	0.267	0.326	0.267	0.334	<u>0.255</u>	<u>0.315</u>	0.305	0.349	0.327	0.371	1.410	0.810
ECL	0.159	<u>0.253</u>	0.167	0.263	0.166	0.264	<u>0.162</u>	0.253	0.214	0.327	0.227	0.338	0.311	0.397
Traffic	<u>0.401</u>	<u>0.273</u>	0.414	0.295	0.434	0.295	0.391	0.264	0.610	0.376	0.628	0.379	0.764	0.416
Avg. Rank	1.286	1.429	3.286	3.000	3.714	3.714	<u>1.714</u>	<u>1.857</u>	5.000	5.000	6.000	6.000	7.000	7.000

Table 3: Few-shot long-term forecasting using 10% and 5% of the training data. For most datasets, results are averaged over prediction lengths $T_{out} \in \{96, 192, 336, 720\}$. However, for datasets marked with * (ETTh1, ETTh2, and Traffic) in the 5% setting, only $T_{out} \in \{96, 192, 336\}$ are used because there are insufficient data to constitute a training set when $T_{out} = 720$. The best average results are in **bold**, while the second-best are underlined.

(a) Few-shot long-term forecasting using 10% of the training data.

Methods	LLM4TS		GPT4TS		DLinear		PatchTST		FEDformer		Autoformer		Informer	
Metric	MSE	MAE	MSE	MAE	MSE	MAE	MSE	MAE	MSE	MAE	MSE	MAE	MSE	MAE
Weather	0.235	0.270	<u>0.238</u>	<u>0.275</u>	0.241	0.283	0.242	0.279	0.284	0.324	0.300	0.342	0.597	0.495
ETTh1	0.525	0.493	<u>0.590</u>	<u>0.525</u>	0.691	0.600	0.633	0.542	0.639	0.561	0.702	0.596	1.199	0.809
ETTh2	0.366	0.407	<u>0.397</u>	<u>0.421</u>	0.605	0.538	0.415	0.431	0.466	0.475	0.488	0.499	3.872	1.513
ETTh1	0.408	0.413	0.464	0.441	<u>0.411</u>	<u>0.429</u>	0.501	0.466	0.722	0.605	0.802	0.628	1.192	0.821
ETTh2	0.276	0.324	<u>0.293</u>	<u>0.335</u>	0.316	0.368	0.296	0.343	0.463	0.488	1.342	0.930	3.370	1.440
ECL	0.172	0.264	<u>0.176</u>	<u>0.269</u>	0.180	0.280	0.180	0.273	0.346	0.427	0.431	0.478	1.195	0.891
Traffic	<u>0.432</u>	0.303	0.440	0.310	0.447	0.313	0.430	<u>0.305</u>	0.663	0.425	0.749	0.446	1.534	0.811
Avg. Rank	1.143	1.000	<u>2.286</u>	<u>2.286</u>	3.857	4.286	3.143	3.000	4.714	4.714	5.857	5.714	7.000	7.000

(b) Few-shot long-term forecasting using 5% of the training data.

Methods	LLM4TS		GPT4TS		DLinear		PatchTST		FEDformer		Autoformer		Informer	
Metric	MSE	MAE	MSE	MAE	MSE	MAE	MSE	MAE	MSE	MAE	MSE	MAE	MSE	MAE
Weather	0.256	0.292	<u>0.264</u>	<u>0.302</u>	0.264	0.309	0.270	0.304	0.310	0.353	0.311	0.354	0.584	0.528
ETTh1*	0.651	0.551	0.682	<u>0.560</u>	0.750	0.611	0.695	0.569	<u>0.659</u>	0.562	0.722	0.599	1.225	0.817
ETTh2*	0.359	0.405	<u>0.401</u>	<u>0.434</u>	0.828	0.616	0.439	0.448	0.441	0.457	0.470	0.489	3.923	1.654
ETTh1	0.413	0.417	0.472	0.450	0.401	0.417	0.527	0.476	0.731	0.593	0.796	0.621	1.163	0.792
ETTh2	0.286	0.332	<u>0.308</u>	<u>0.346</u>	0.399	0.426	0.315	0.353	0.381	0.405	0.389	0.434	3.659	1.490
ECL	0.173	0.266	0.179	<u>0.273</u>	<u>0.177</u>	0.276	0.181	0.277	0.267	0.353	0.346	0.405	1.281	0.930
Traffic*	0.418	0.295	0.434	0.305	0.451	0.317	0.418	<u>0.297</u>	0.677	0.424	0.833	0.502	1.591	0.832
Avg. Rank	1.143	1.000	<u>2.571</u>	<u>2.286</u>	4.000	4.143	3.429	3.286	4.286	4.429	5.571	5.714	7.000	7.000

al., 2021], and Informer [Zhou *et al.*, 2021] are recognized as train-from-scratch time-series forecasting models. The same set of models is used for few-shot learning and ablation studies. For self-supervised learning, we choose PatchTST, BTSF [Yang and Hong, 2022], TS2Vec [Yue *et al.*, 2022], TNC [Tonekaboni *et al.*, 2021], and TS-TCC [Eldele *et al.*, 2021]. Consistent with prior research [Zhou *et al.*, 2023], we rely on Mean Squared Error (MSE) and Mean Absolute Error (MAE) as evaluation metrics across all experiments.

Implementation Details For our experiments in long-term time-series forecasting, few-shot learning, and ablation studies, we use the configurations from PatchTST [Nie *et al.*, 2023] for a consistent comparison. We set our look-back

window length T_{in} to either 336 or 512 (reporting the best results), and configure the patch length P as 16 with a stride S of 8. For self-supervised learning, the settings are slightly adjusted to $T_{in} = 512$, $P = 12$, and $S = 12$. Aligned with the GPT4TS configuration [Zhou *et al.*, 2023], we utilize only the first 6 layers of the 12-layer GPT-2 base [Radford *et al.*, 2019]. For the LP-FT training strategy in the forecasting fine-tuning stage, the initial half of the epochs is dedicated to linear probing, while the latter half focuses on full fine-tuning.

5.1 Long-Term Time-Series Forecasting

Table 2 presents the results of long-term time-series forecasting averaged over a consistent prediction length set $T_{out} \in \{96, 192, 336, 720\}$ for all datasets. For each dataset, we

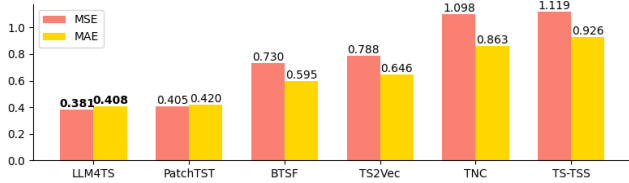


Figure 4: Self-supervised learning evaluation in forecasting with linear evaluation. We use results averaged over prediction lengths $T_{out} \in \{24, 48, 168, 336, 720\}$ for the ETTh1 dataset. The best average results are in **bold**.

train a single model in the time-series alignment stage, which is then applied consistently across all prediction lengths. In contrast, in the forecasting fine-tuning stage, we train a distinct model for each prediction length, while ensuring that all these models share the same hyperparameters. Although the primary intent of using the pre-trained LLM is for few-shot learning, LLM4TS still surpasses all baseline methods even when given access to the full dataset. By using two-stage fine-tuning and incorporation of multi-scale temporal information, LLM4TS achieves the highest rank in 9 of the 14 evaluations, covering 7 datasets and 2 metrics.

5.2 Few-Shot Learning

Table 3 shows the results of using only 10% and 5% of the training data in long-term time-series forecasting. In our experiments, we maintain consistent splits for training, validation, and test sets in both full- and few-shot learning, and in few-shot scenarios, we intentionally limit the training data percentage. Both LLM4TS and GPT4TS [Zhou *et al.*, 2023] consistently surpass most train-from-scratch models in limited-data scenarios across various datasets, thanks to the pre-existing representation learning capability encapsulated in GPT-2. Notably, LLM4TS with only 5% of data outperforms the best baseline that uses 10% of data.

5.3 Self-Supervised Learning

Given that the autoregressive objective used in the time-series alignment stage can be seen as a pretext task in self-supervised learning, we aim to assess LLM4TS’s representation learning capability. To evaluate the effectiveness of self-supervised learning, we conduct a linear evaluation on time-series forecasting. This involves pre-training the backbone model using the pretext task, freezing its weights, and then training an attached linear layer on the downstream forecasting task. With the backbone model’s parameters fixed, strong performance in forecasting depends on the expressiveness of the learned representations. Figure 4 shows LLM4TS’s superior performance over competitors on the ETTh1 dataset, highlighting the effectiveness of adapting the LLM to time-series characteristics in the time-series alignment stage.

5.4 Ablation Study

Key Components in LLM4TS

Figure 5a explores the effects of time-series alignment, temporal encoding, and PEFT in LLM4TS, assessing both full- and few-shot scenarios on the ETTh1 dataset. A comparative

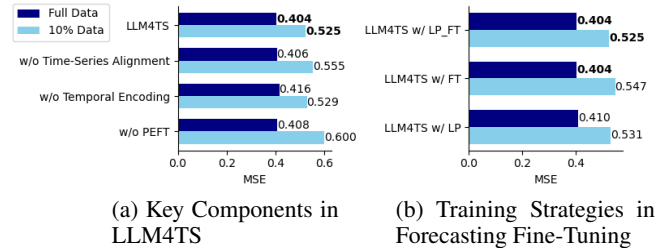


Figure 5: Ablation study. Each ablation is conducted under both full- and few-shot learning with 10% training data. We use results averaged over prediction lengths $T \in \{96, 192, 336, 720\}$ for the ETTh1 dataset. The best average results are in **bold**.

analysis—with and without these components—highlights their individual importance in enhancing forecasting accuracy in both scenarios. Notably, LLM4TS delivers exceptional performance in few-shot learning, averaging a 6.2% reduction in MSE with each incorporation of these components.

Training Strategies in Forecasting Fine-Tuning

As discussed in Section 4.2, while full fine-tuning (FT) shows superior performance in out-of-distribution (OOD) scenarios and linear probing (LP) excels in in-distribution (ID) scenarios, LP-FT can surpass FT and LP in both OOD and ID scenarios. Figure 5b shows that LP-FT enhances performance in both full- and few-shot learning on the ETTh1 dataset, achieving an average improvement of 0.7% in MSE for full-shot learning and 2.51% for few-shot learning. The subtle improvements in both scenarios can be attributed to the limited number of trainable parameters in the LLM4TS’s backbone model even when using FT, which narrows the distinction between LP and FT. Notably, few-shot learning benefits more from LP-FT than full-shot learning, mainly because it is more susceptible to severe OOD issues.

6 Conclusion

In this paper, we present LLM4TS, a framework for time-series forecasting utilizing pre-trained LLMs. LLM4TS employs a two-stage fine-tuning strategy, beginning with the *time-series alignment* stage to adapt LLMs to the characteristics of time-series data, followed by the *forecasting fine-tuning* stage designed for time-series forecasting tasks. Our framework also introduces a novel two-level aggregation method, integrating multi-scale temporal data within pre-trained LLMs to improve their interpretation of time-related information. Through experiments on 7 time-series forecasting datasets, LLM4TS demonstrates superior performance over existing state-of-the-art methods, including those trained from scratch, in both full and few-shot scenarios.

In future work, we plan to extend our research in two directions. First, we plan to evaluate newer LLMs like GPT-3 and LLaMA-2, expanding on our use of GPT-2 to assess improvements over GPT4TS. Second, we aim to explore other tasks, such as classification and anomaly detection. Although forecasting is highly relevant to real-world applications without the need for manual labeling, extending it to other tasks ensures the broader applicability of our LLM4TS framework.

References

- [Chang *et al.*, 2023] Ching Chang, Chiao-Tung Chan, Wei-Yao Wang, Wen-Chih Peng, and Tien-Fu Chen. Time-drl: Disentangled representation learning for multivariate time-series. *arXiv preprint arXiv:2312.04142*, 2023.
- [Eldele *et al.*, 2021] Emadeldeen Eldele, Mohamed Ragab, Zhenghua Chen, Min Wu, C. Kwok, Xiaoli Li, and Cuntai Guan. Time-series representation learning via temporal and contextual contrasting. In *International Joint Conference on Artificial Intelligence*, 2021.
- [Ghosal *et al.*, 2023] Deepanway Ghosal, Navonil Majumder, Ambuj Mehri, and Soujanya Poria. Text-to-audio generation using instruction-tuned llm and latent diffusion model. *ArXiv*, abs/2304.13731, 2023.
- [Giannou *et al.*, 2023] Angeliki Giannou, Shashank Rajput, Jy-yong Sohn, Kangwook Lee, Jason D Lee, and Dimitris Papailiopoulos. Looped transformers as programmable computers. *arXiv preprint arXiv:2301.13196*, 2023.
- [Hegselmann *et al.*, 2023] Stefan Hegselmann, Alejandro Buendia, Hunter Lang, Monica Agrawal, Xiaoyi Jiang, and David Sontag. Tabllm: Few-shot classification of tabular data with large language models. In *International Conference on Artificial Intelligence and Statistics*, pages 5549–5581. PMLR, 2023.
- [Hoffmann *et al.*, 2022] Jordan Hoffmann, Sebastian Borgeaud, Arthur Mensch, Elena Buchatskaya, Trevor Cai, Eliza Rutherford, Diego de Las Casas, Lisa Anne Hendricks, Johannes Welbl, Aidan Clark, et al. Training compute-optimal large language models. *arXiv preprint arXiv:2203.15556*, 2022.
- [Hu *et al.*, 2021] Edward J Hu, Yelong Shen, Phillip Wallis, Zeyuan Allen-Zhu, Yuanzhi Li, Shean Wang, Lu Wang, and Weizhu Chen. Lora: Low-rank adaptation of large language models. *arXiv preprint arXiv:2106.09685*, 2021.
- [Kim *et al.*, 2021] Taesung Kim, Jinhee Kim, Yunwon Tae, Cheonbok Park, Jang-Ho Choi, and Jaegul Choo. Reversible instance normalization for accurate time-series forecasting against distribution shift. In *International Conference on Learning Representations*, 2021.
- [Kumar *et al.*, 2022] Ananya Kumar, Aditi Raghunathan, Robbie Jones, Tengyu Ma, and Percy Liang. Fine-tuning can distort pretrained features and underperform out-of-distribution. *arXiv preprint arXiv:2202.10054*, 2022.
- [Lai *et al.*, 2018] Guokun Lai, Wei-Cheng Chang, Yiming Yang, and Hanxiao Liu. Modeling long-and short-term temporal patterns with deep neural networks. In *The 41st international ACM SIGIR conference on research & development in information retrieval*, pages 95–104, 2018.
- [Liu *et al.*, 2021] Minghao Liu, Shengqi Ren, Siyuan Ma, Jiahui Jiao, Yizhou Chen, Zhiguang Wang, and Wei Song. Gated transformer networks for multivariate time series classification. *arXiv preprint arXiv:2103.14438*, 2021.
- [Lu *et al.*, 2021] Kevin Lu, Aditya Grover, Pieter Abbeel, and Igor Mordatch. Pretrained transformers as universal computation engines. *arXiv preprint arXiv:2103.05247*, 1, 2021.
- [Nie *et al.*, 2023] Yuqi Nie, Nam H. Nguyen, Phanwadee Sinthong, and Jayant Kalagnanam. A time series is worth 64 words: Long-term forecasting with transformers. In *ICLR*. OpenReview.net, 2023.
- [Radford *et al.*, 2019] Alec Radford, Jeffrey Wu, Rewon Child, David Luan, Dario Amodei, Ilya Sutskever, et al. Language models are unsupervised multitask learners. *OpenAI blog*, 1:9, 2019.
- [Tonekaboni *et al.*, 2021] Sana Tonekaboni, Danny Eytan, and Anna Goldenberg. Unsupervised representation learning for time series with temporal neighborhood coding. In *ICLR*. OpenReview.net, 2021.
- [Touvron *et al.*, 2023] Hugo Touvron, Thibaut Lavril, Gautier Izacard, Xavier Martinet, Marie-Anne Lachaux, Timothée Lacroix, Baptiste Rozière, Naman Goyal, Eric Hambro, Faisal Azhar, Aurelien Rodriguez, Armand Joulin, Edouard Grave, and Guillaume Lample. Llama: Open and efficient foundation language models. *ArXiv*, abs/2302.13971, 2023.
- [Wu *et al.*, 2021] Haixu Wu, Jiehui Xu, Jianmin Wang, and Mingsheng Long. Autoformer: Decomposition transformers with auto-correlation for long-term series forecasting. *Advances in Neural Information Processing Systems*, 34:22419–22430, 2021.
- [Xu *et al.*, 2021] Jiehui Xu, Haixu Wu, Jianmin Wang, and Mingsheng Long. Anomaly transformer: Time series anomaly detection with association discrepancy. *arXiv preprint arXiv:2110.02642*, 2021.
- [Yang and Hong, 2022] Ling Yang and Shenda Hong. Unsupervised time-series representation learning with iterative bilinear temporal-spectral fusion. In *International Conference on Machine Learning*, pages 25038–25054. PMLR, 2022.
- [Yeh *et al.*, 2019] Cheng-Han Yeh, Yao-Chung Fan, and Wen-Chih Peng. Interpretable multi-task learning for product quality prediction with attention mechanism. In *2019 IEEE 35th International Conference on Data Engineering (ICDE)*, pages 1910–1921. IEEE, 2019.
- [Yue *et al.*, 2022] Zhihan Yue, Yujing Wang, Juanyong Duan, Tianmeng Yang, Congrui Huang, Yunhai Tong, and Bixiong Xu. Ts2vec: Towards universal representation of time series. In *Proceedings of the AAAI Conference on Artificial Intelligence*, volume 36, pages 8980–8987, 2022.
- [Zeng *et al.*, 2023] Ailing Zeng, Muxi Chen, Lei Zhang, and Qiang Xu. Are transformers effective for time series forecasting? In *Proceedings of the AAAI conference on artificial intelligence*, volume 37, pages 11121–11128, 2023.
- [Zhang *et al.*, 2022] Xiang Zhang, Ziyuan Zhao, Theodoros Tsiligkaridis, and Marinka Zitnik. Self-supervised contrastive pre-training for time series via time-frequency consistency. *Advances in Neural Information Processing Systems*, 35:3988–4003, 2022.

- [Zhou *et al.*, 2021] Haoyi Zhou, Shanghang Zhang, Jieqi Peng, Shuai Zhang, Jianxin Li, Hui Xiong, and Wancai Zhang. Informer: Beyond efficient transformer for long sequence time-series forecasting. In *Proceedings of the AAAI conference on artificial intelligence*, volume 35, pages 11106–11115, 2021.
- [Zhou *et al.*, 2022] Tian Zhou, Ziqing Ma, Qingsong Wen, Xue Wang, Liang Sun, and Rong Jin. Fedformer: Frequency enhanced decomposed transformer for long-term series forecasting. In *International Conference on Machine Learning*, pages 27268–27286. PMLR, 2022.
- [Zhou *et al.*, 2023] Tian Zhou, Peisong Niu, Xue Wang, Liang Sun, and Rong Jin. One fits all: Power general time series analysis by pretrained lm. *arXiv preprint arXiv:2302.11939*, 2023.